



The Pampean region (Argentina) underwent larger variation in aridity than in temperature during the late Pleistocene: New evidence from the isotopic analysis of mammalian taxa

Dánae Sanz-Pérez ^{a, b, *}, Manuel Hernández Fernández ^{a, b}, Rodrigo L. Tomassini ^c,
Claudia I. Montalvo ^d, Elisa Beilinson ^e, Germán M. Gasparini ^f, Laura Domingo ^{a, b, g}

^a Departamento de Geodinámica, Estratigrafía y Paleontología, Facultad Ciencias Geológicas, Universidad Complutense de Madrid, 28040, Madrid, Spain

^b Departamento de Geología Sedimentaria y Cambio Medioambiental, Instituto de Geociencias (CSIC, UCM), 28040, Madrid, Spain

^c INGEOSUR, Departamento de Geología, Universidad Nacional del Sur (UNS)-CONICET, 8000, Bahía Blanca, Argentina

^d Facultad de Ciencias Exactas y Naturales, Universidad Nacional de La Pampa, 6300, Santa Rosa, Argentina

^e Centro de Investigaciones Geológicas (CONICET-UNLP), Diag. 113 # 275, 1900, La Plata, Argentina

^f División Paleontología Vertebrados, Unidades de Investigación Anexo Museo de La Plata, Facultad de Ciencias Naturales y Museo, UNLP. CONICET. 122 y 60, 1900, La Plata, Argentina

^g Earth and Planetary Sciences Department, University of California Santa Cruz, 95064, Santa Cruz, California, USA

ARTICLE INFO

Article history:

Received 31 December 2021

Received in revised form

8 April 2022

Accepted 3 May 2022

Available online xxx

Handling Editor: Danielle Schreve

Keywords:

Quaternary

Fossil mammals

Southern south America

Stable isotopes

Palaeoclimatology

Palaeoecology

Precipitation

Glacial-interglacial variability

ABSTRACT

During the Pleistocene intense climatic changes occurred corresponding with the alternation of interglacial and glacial periods. By means of stable isotope analysis on fossil mammals, this research allows the assessment of the palaeoecological and palaeoclimatic conditions, including the possible scenarios for the atmospheric circulation pattern during three key phases of the late Pleistocene in the Pampean region of Argentina: Last Interglacial (LIG, MIS 5e; unpublished data), Last Glacial Maximum (LGM; 28,170–19,849 cal BP yrs), and post-Last Glacial Maximum (post-LGM, 17,281–11,500 cal BP yrs). Tooth enamel $\delta^{13}\text{C}$ values of mammals from the Last Glacial Maximum showed an increase in C_4 plants consumption compared to the other two phases studied, which may be related to a reduction in forest cover due to a combination of environmental factors such as decreased pCO_2atm and increased aridity. We evaluated mean annual precipitation (MAP) and mean annual temperature (MAT) variability from tooth enamel $\delta^{13}\text{C}$ and $\delta^{18}\text{O}$ values, which showed a greater variation in precipitation between phases than in temperature. This result enabled us to propose two climate regimes for the studied temporal sequence, an arid-temperate regime, and a humid-temperate regime, which were mostly regulated by variations in atmospheric circulation.

© 2022 The Authors. Published by Elsevier Ltd. This is an open access article under the CC BY-NC-ND license (<http://creativecommons.org/licenses/by-nc-nd/4.0/>).

1. Introduction

The Quaternary (2.588 ± 0.04 Ma – present) is characterised by cyclical climatic changes corresponding to alternating temperate-warm (interglacial phases) and cold (glacial phases) periods,

* Corresponding author. Departamento de Geodinámica, Estratigrafía y Paleontología, Facultad Ciencias Geológicas, Universidad Complutense de Madrid, 28040, Madrid, Spain.

E-mail addresses: dasanz01@ucm.es (D. Sanz-Pérez), hdezfdz@ucm.es (M. Hernández Fernández), rodrigo.tomassini@yahoo.com.ar (R.L. Tomassini), cmontalvo@exactas.unlpam.edu.ar (C.I. Montalvo), elisabeilinson@gmail.com (E. Beilinson), germanmgasparini@gmail.com (G.M. Gasparini), ldomingo@ucm.es (L. Domingo).

during which the extinction of several large mammals and all megamammals occurred in South America. The study of the last interglacial-glacial cycle provides a solid framework for understanding changes in vegetation, faunal behaviour, palaeogeography, and climate, among others. Numerous studies have evaluated glacial and interglacial phases in the Northern Hemisphere (e.g. Richmond and Fullerton, 1986; Kershaw and Whitlock, 2000; Hernández Fernández, 2006; Antoine et al., 2013; Yehudai et al., 2021), while a much lower number have focused on the Southern Hemisphere (e.g. Hulton et al., 2002; Glasser et al., 2004; Mayle et al., 2004; Ward et al., 2015).

Different climatic zones are currently recognised in southern South America (Beck et al., 2018), which are modulated by the

influence of atmospheric circulation. Since the Pleistocene (2.58 ± 0.04), the Pampean region of Argentina has been interpreted as an ecotonal area between arid (Patagonia) and humid (Brazil) zones (García-Morato et al., 2021). Precipitation and the influence of cold/dry or warm/wet winds in this region are controlled by the subtropical jet stream, the southern westerly winds and the high-pressure systems of the South Atlantic and South Pacific oceans (Iriando and García, 1993; Prieto, 1996; Gallego et al., 2005; Garreaud et al., 2009; Romero et al., 2021). Variation in the global atmospheric circulation pattern during the last glacial phase (late Pleistocene), effected the past and currently climate conditions of this region, with a colder and drier climate (Quattrocchio et al., 2008).

In this scenario, we aim to increase the knowledge on the last interglacial-glacial cycle in austral South America. Our main goal is to evaluate the climatic and environmental trends throughout late Pleistocene in the Pampean region by stable isotope analysis on mammalian fossils. Analysing the bioapatite stable isotope variability of mammal species in a specific region under a time range allows interpretation on palaeoclimatic, palaeoecological, and palaeogeographical conditions. Here, we provide the first comparative study mammalian isotopic data from different localities at three key moments of the glacial-interglacial alternation in South America: Last Interglacial (LIG, MIS 5e; unpublished data), Last Glacial Maximum (LGM, 28,170 to 19,848 cal BP years) and post-Last Glacial Maximum (post-LGM, 17,281 to 11,5 cal BP years).

Carbon isotope values have been used to characterise the diet and habitat preferences of species, as well as to calculate mean annual precipitations. The $\delta^{13}\text{C}$ values from herbivores diets depend on the ingested vegetation, which are controlled by the photosynthetic pathway of plants (Farquhar et al., 1989; Koch, 1998; Hayes, 2001). Trees, shrubs, forbs, and cool-season grasses follow the C_3 photosynthetic pathway, which has a considerable range in $\delta^{13}\text{C}$ between -36 and -22‰ (VPDB) (Cerling et al., 1997; Domingo et al., 2012). C_4 grasses and sedges from regions with a warm growing season and summer precipitation follow the C_4 photosynthetic pathway, which has a more restricted $\delta^{13}\text{C}$ range between -17 and -9‰ (Cerling et al., 1997; Koch, 1998; Domingo et al., 2012; Hynek et al., 2012). Succulent plants follow the CAM (Crassulacean Acid Metabolism) pathway showing intermediate isotopic values between those of C_3 and C_4 plants (Cerling et al., 1997; Domingo et al., 2012).

Oxygen isotope values of carbonate and phosphate fractions of tooth enamel bioapatite record the $\delta^{18}\text{O}$ value of body water, resulted by a combination of oxygen entering and exiting the body (Domingo et al., 2012). It should be noted that there are differences between obligate (they obtain most of their water from drinking) and non-obligate (they mainly obtain water from plant water and metabolic water) drinkers (Kohn, 1996; Domingo et al., 2009; 2012). The $\delta^{18}\text{O}$ value of obligate drinker animals is determined by the isotopic composition of the water drunk. $\delta^{18}\text{O}$ values are useful in palaeoclimatic, palaeoenvironmental and palaeoecological reconstructions since changes in the $\delta^{18}\text{O}$ values of the same taxon reflect isotopic variation of water conditions (Koch, 2007). These variations depend on different climatic and geographic variables, such as annual temperature, evaporation rate (humidity/aridity levels), precipitation amount, latitude, altitude, and distance of the fossil site to the coast (Dansgaard, 1964; Luz et al., 1990; Araguás-Araguás et al., 2000; Domingo et al., 2017).

In order to carry out the palaeoclimatic and palaeoenvironmental study of the late Pleistocene in the Pampean region, we (i) analysed the palaeoecological dynamics of the LIG and LGM fossil sites, providing also a slight discussion on the post-LGM

period, (ii) performed a palaeoclimatic assessment through time, (iii) evaluated the relevance of C_4 vegetation during the LGM, and (iv) established potential scenarios for the atmospheric circulation pattern associated with glacial and interglacial phases.

2. Material and methods

We analysed mammalian tooth enamel and orthodontine samples from nine fossil sites located in the Pampean region of Argentina spanning from $\sim 128,000$ – $116,000$ cal BP years (MIS 5e, unpublished data; see Stirling et al., 1998) to $\sim 11,500$ cal BP years (late Pleistocene) and grouped in the three mentioned climatic phases (LIG, LGM and post-LGM) (Fig. 1). The stable carbon and oxygen isotope composition on the carbonate fraction of bioapatite ($\delta^{13}\text{C}$ and $\delta^{18}\text{O}_{\text{CO}_3}$, respectively) was determined for litopterns, notoungulates, cingulates, pilosans, artiodactyls, perissodactyls and proboscideans. The sampled fossil teeth are housed in the Universidad Nacional del Centro de la Provincia de Buenos Aires (FCS; Olavarría, Buenos Aires, Argentina), Facultad de Ciencias Exactas y Naturales de la Universidad Nacional de La Pampa (GHUNLPam; Santa Rosa, La Pampa, Argentina), Museo Argentino de Ciencias Naturales “Bernardino Rivadavia” (MACN; Buenos Aires, Buenos Aires, Argentina), Museo Municipal de Ciencias Naturales “Carlos Darwin” (MD-PDB; Punta Alta, Buenos Aires, Argentina), Museo Municipal de Ciencias Naturales “Vicente Di Martino” (MMH-QEQ; Monte Hermoso, Buenos Aires, Argentina) and Museo de La Plata (MLP; La Plata, Buenos Aires, Argentina).

We evaluated data from tooth enamel and orthodontine samples available in previous works (Table A1). Specifically, 116 carbonate samples and 99 phosphate samples in bioapatite were used for this study. Tooth enamel and orthodontine were sampled using a rotary drill with a diamond-tipped dental burr, from an area of the tooth as large as possible to avoid seasonal bias from the time of mineralization. Chemical treatment followed the methodology described in Domingo et al. (2013). The carbon and oxygen isotope results are reported in δ -notation, $\delta^{\text{H}}\text{X}_{\text{sample}} = [(R_{\text{sample}} - R_{\text{standard}})/R_{\text{standard}}] \times 1000$, where X is the element, H is the mass of the rare, heavy isotope and $R = {}^{13}\text{C}/{}^{12}\text{C}$ or ${}^{18}\text{O}/{}^{16}\text{O}$. Vienna Pee Dee Belemnite (VPDB) is the standard for $\delta^{13}\text{C}$ values, whereas Vienna Standard Mean Ocean Water (VSMOW) is the standard for $\delta^{18}\text{O}$ values (Hoefs, 1997).

When assessing the diet of herbivorous mammals, a diet-enamel fractionation ($\epsilon^{\text{diet-enamel}}$), associated with carbonate balances and metabolic processes, must be considered (Cerling and Harris, 1999; Passey et al., 2005). In this study, we follow the methodology of Domingo et al. (2020) who use different $\epsilon^{\text{diet-enamel}}$ values for the $\delta^{13}\text{C}$ cut-off ranges of vegetation proposed by other authors depending on the taxa (ungulates or xenarthrans). For ungulates, we followed the $\epsilon^{\text{diet-enamel}}$ of $+14.1\text{‰}$ proposed by Cerling and Harris (1999). Therefore, in this case of ungulates, the $\delta^{13}\text{C}$ boundary between C_3 -dominated diet and intermediate C_3 – C_4 diet is considered between $\sim -9\text{‰}$ to -8‰ , whereas between intermediate C_3 – C_4 diet and C_4 -dominated diet is considered between $\sim -2\text{‰}$ to -1‰ . Based on the estimated dietary-bioapatite $\delta^{13}\text{C}$ enrichment for the extinct ground sloth *Myodon darwini* proposed by Tejada-Lara et al. (2018), an $\epsilon^{\text{diet-enamel}}$ of $+15.6\text{‰}$ is used for xenarthrans. Therefore, we consider the $\delta^{13}\text{C}$ boundary between C_3 -dominated diet and intermediate C_3 – C_4 diet as $\sim -7\text{‰}$ to -6‰ , whereas the $\delta^{13}\text{C}$ boundary between intermediate C_3 – C_4 diet and C_4 -dominated diet as $\sim 0\text{‰}$ – 1‰ .

R software version 4.0.3 (R Core Team, 2019) was used for statistical analysis and graphical representation of the isotopic results. Shapiro-Wilk tests demonstrated the normal distribution of the

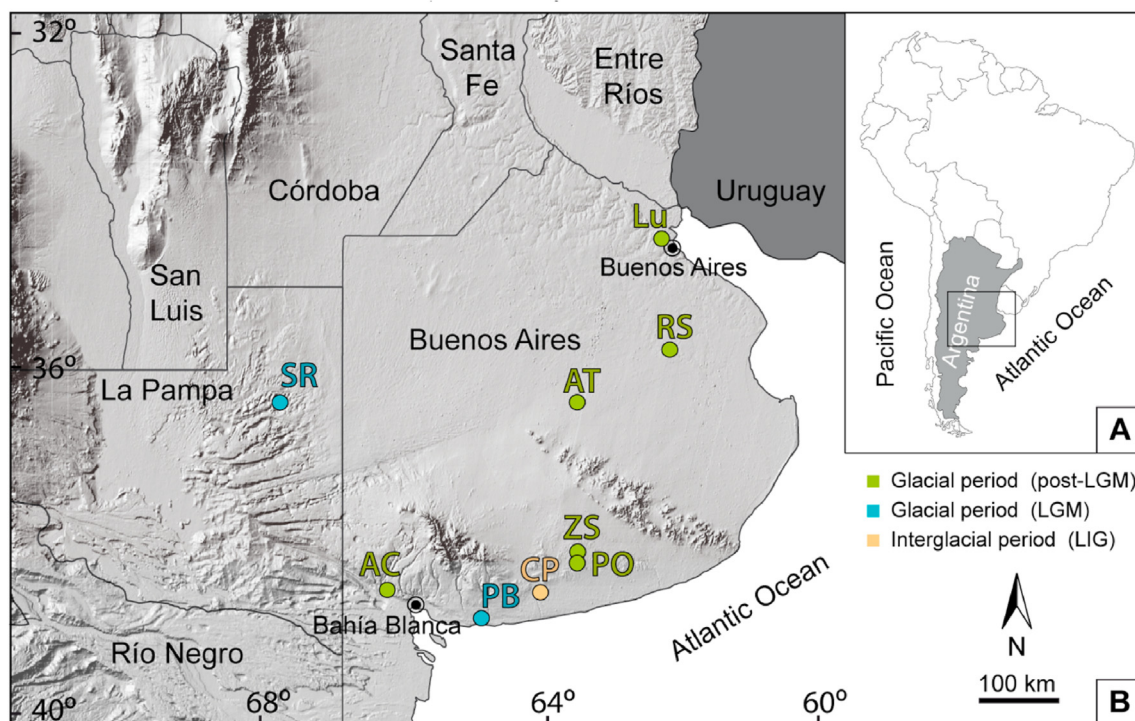


Fig. 1. Geographical setting of the studied palaeontological localities. (A) General map of South America. (B) Map of the Late Pleistocene sites of the Argentinean Pampean region (La Pampa and Buenos Aires provinces) selected in this study. AC: Arroyo Chasicó, AT: Arroyo Tapalqué, CP: Cascada del Paleolama, Lu: Luján, PB: Playa del Barco, PO: Paso Otero, RS: Río Salado, SR: Santa Rosa, ZS: Zanjón Seco.

isotopic data and, therefore, we performed parametric analyses (ANOVA and post-hoc Tukey analysis) to detect significant differences in the mean of isotopic values among fossil localities and taxa. The significance level was set at $p = 0.05$. Some taxa could not be included in these analyses due to the lack of samples (a minimum of 3 samples is required).

To evaluate the isotopic niches of the late Pleistocene mammals, we used SIBER [Stable Isotope Bayesian Ellipses in R (Jackson et al., 2011)]. The term “isotopic niche” refers to an area (δ -space) with isotope values (δ -values) as coordinates, so the variance in δ -space among individuals is related to realized niche width (Clementz et al., 2009). To assess isotopic niche using SIBER it is necessary to use at least two isotopic systems ($\delta^{13}\text{C}$ and $\delta^{18}\text{O}$, in our case), which allow the delimitation of a 2D δ -space. SIBER also needs to be fed with at least three data points per taxon to retrieve ellipses. SIBER uses a Markov Chain Monte Carlo (MCMC) model-fitting algorithm to construct a standard ellipse area (SEA) that best fits each set of $\delta^{13}\text{C}$ and $\delta^{18}\text{O}$ from different members within a (paleo) community (i.e., different taxa). We evaluated the isotopic niche in those localities with a good representation of taxa (three or more genus) and where each genus has a broad sampling record to retrieve ellipses (three or more samples per genus). This is the case of Cascada del Paleolama, which belongs to the LIG, and Santa Rosa and Playa del Barco, which belong to the LGM (Fig. 1). These three fossil sites have been selected for a more detailed palaeoecological analysis due to the high number of samples and taxa represented. Most localities of the post-LGM phase have only perissodactyl samples and, therefore, had to be discarded for this analysis.

In order to evaluate variability in palaeoenvironmental and palaeoclimatological parameters such as precipitation, aridity patterns, and temperature throughout the LIG, LGM and post-LGM, we select the tooth enamel $\delta^{13}\text{C}$ and $\delta^{18}\text{O}$ values of equids (*Equus* and *Hippidion*) on account of: i) they are obligate drinkers and provide a

reliable record of meteoric/precipitation $\delta^{18}\text{O}$ values and environmental temperature, and ii) they are well represented in the majority of selected localities granting a continuous temporal record.

For the estimation of the mean annual temperature (MAT), the $\delta^{18}\text{O}$ isotopic values of equids have been considered. The $\delta^{18}\text{O}$ value of water ($\delta^{18}\text{O}_{\text{H}_2\text{O}}$) ingested by *Equus* and *Hippidion* were calculated using their $\delta^{18}\text{O}_{\text{PO4}}$ values from the tooth enamel (Table A1). For calculation of $\delta^{18}\text{O}_{\text{H}_2\text{O}}$ values, we followed the equation proposed by Huertas et al. (1995) for modern equivalents of equids. Finally, we used a regression equation between MAT and weighted $\delta^{18}\text{O}_{\text{H}_2\text{O}}$ using the meteorological data included in Dansgaard (1964). In tropical (and some subtropical) areas, with high precipitation rates and high MAT, precipitation $\delta^{18}\text{O}_{\text{H}_2\text{O}}$ values do not correlate with MAT as it happens in temperate climates (i.e., higher MAT corresponds to higher precipitation $\delta^{18}\text{O}_{\text{H}_2\text{O}}$ and vice versa). In tropical regions, the precipitation excess saturates the atmosphere and even at high MAT, there is no preferential removal (via evaporation) of ^{16}O . This translates in a decrease of precipitation $\delta^{18}\text{O}_{\text{H}_2\text{O}}$ even at high MAT due to the “amount effect” (Dansgaard, 1964; Higgins and MacFadden, 2004). In order to avoid databases affected by this effect and since the studied region belongs to a temperate latitude, the equation of Dansgaard (1964) was chosen (i.e., tropical and subtropical areas are relatively scarce and temperate stations predominate).

The mean annual precipitation (MAP) was estimated from the $\delta^{13}\text{C}$ values of equids following Kohn (2010). This work shows that diets with high C_4 plant consumption cannot be considered in MAP reconstructions since the high value of $\delta^{13}\text{C}_{\text{diet}}$ reflects low or negative MAP values. Therefore, the MAP estimate is evidence of C_4 plant consumption and not of aridity. Equids present a mixed C_3 – C_4 diet in some sites, therefore, values from cervids with a pure C_3 diet were used where possible (i.e. Playa del Barco). The estimation of MAP implies that a modern equivalent of the diet (vegetation)

composition ($\delta^{13}\text{C}_{\text{diet,meq}}$) must be first calculated using the equation:

$$\delta^{13}\text{C}_{\text{diet,meq}} = \delta^{13}\text{C}_{\text{leaf}} + (\delta^{13}\text{C}_{\text{modernatmCO}_2} - \delta^{13}\text{C}_{\text{ancientatmCO}_2}) \text{ (Kohn, 2010)}$$

where $\delta^{13}\text{C}_{\text{leaf}} = \delta^{13}\text{C}_{\text{tooth}} - 14.1\text{‰}$ (Cerling and Harris, 1999), $\delta^{13}\text{C}_{\text{modernatmCO}_2}$ is -8‰ and $\delta^{13}\text{C}_{\text{ancientatmCO}_2}$ values for different time periods are taken from Koch et al. (2004). We also used $\delta^{13}\text{C}$ values to estimate the proportion of C_4 plants in the equid diet with a mass balance equation proposed by Koch et al. (2004).

3. Results and discussion

3.1. Palaeoecology across the last interglacial and the Last Glacial Maximum

In order to analyse palaeoecological variability (or lack thereof) across the Last Interglacial and the Last Glacial Maximum, three fossil sites were selected: Cascada del Paleolama (LIG), Santa Rosa, and Playa del Barco (both belonging to the LGM). The reasons for this selection are: i) they record a diverse mammalian assemblage, ii) they have a significant amount of bioapatite samples, and iii) they have dating. A summary of the isotopic mean, standard deviation values, and other additional information, of these localities is shown in Table 1.

3.1.1. Cascada del Paleolama (LIG)

The total $\delta^{13}\text{C}$ values of Cascada del Paleolama point to a combination of wooded C_3 grassland and open intermediate C_3 – C_4 areas (Fig. 2). It can be observed that the equid *Equus* recorded both the lowest (-10.1‰) and the highest (-3.3‰) values of the taxon dataset (Table A1). These values point to a flexible dietary behaviour for this taxon, which would have included individuals with both pure- C_3 and mixed C_3 – C_4 plants consumption (Fig. 2). These results agree with $\delta^{13}\text{C}$ values obtained for other samples of *Equus* from different regions of South America (MacFadden, 2005). The ellipse $\delta^{13}\text{C}$ – $\delta^{18}\text{O}$ could not be recovered for *Hippidion*, the other equid represented, as it has less than three points, but the data fall within the area of mixed C_3 – C_4 vegetation (Fig. 2). Numerous studies have found that the litoptern *Macrauchenia* was probably a mixed feeder (MacFadden and Shockey, 1997; Domingo et al., 2012; Bocherens et al., 2016; de Oliveira et al., 2021) and our results are consistent with an intermediate C_3 – C_4 plants-based diet. The camelid *Hemiauchenia* and the notoungulate *Toxodon* have a mixed C_3 – C_4 diet although they incorporated plants from C_3 dominated open areas in their diets. Some studies indicate that *Toxodon* had an exclusive C_3 diet (e.g. Argentina, Domingo et al., 2012; Bocherens et al., 2016) while others infer a preference for C_4 plants (e.g. Southern and Midwest Brazil, Lopes et al., 2013; Pansani et al., 2019). From a palaeoecological point of view, these results indicate that *Toxodon* was possibly a generalist taxon, and its dietary preference would be related to the ecological pressures of each environment and/or temporal period. The camelid *Lama* and the cervid *Morenelaphus* showed $\delta^{13}\text{C}$ values that evidence a C_3 plant-based diet, but lower isotopic values in the case of the latter may be related to consumption of food items from more wooded environments. There were no statistically significant differences among taxa from this locality (ANOVA, $F = 0.311$, $p = 0.736$, Table A2), but *Lama* and *Morenelaphus* (lowest $\delta^{13}\text{C}$ values) were not included in the analysis due to the shortage of isotopic data.

$\delta^{18}\text{O}$ values ranged between 28.0‰ (*Equus*) and 32.6‰ (*Lama*) (Table A1). No significant differences were obtained among taxa (ANOVA, $F = 2.307$, $p = 0.127$, Table A2), pointing to the consumption of water with similar $\delta^{18}\text{O}$ content and therefore, subject

to a similar hydrological regime. Whereas the $\delta^{18}\text{O}$ data of *Lama* was not considered in statistical tests, we can observe that their high $\delta^{18}\text{O}$ values suggest the intake of water that underwent higher evaporation, probably leaf water. Loponte and Corriale (2020)'s isotopic study of living *Lama guanicoe* from the Pampean region, particularly the Rolling Pampa (Pampa Ondulada, Buenos Aires Province) revealed its high $\delta^{18}\text{O}$ values ($0.12 \pm 0.6\text{‰}$). This is probably related to a predominant water intake from enriched streams and shallow lakes. In addition, the ingestion of leaves, which also have enriched oxygen values compared to meteoric waters, may explain these values.

3.1.2. Santa Rosa and Playa del Barco (LGM)

$\delta^{13}\text{C}$ values from Santa Rosa indicate intermediate C_3 – C_4 diet for all taxa except the xenarthran megatheriid *Megatherium*, which consumed exclusively C_3 plants from open areas (Fig. 2). The minimum value of $\delta^{13}\text{C}$ of -8.7‰ corresponds to a sample of *Megatherium* and the maximum of -2.2‰ to a sample of the xenarthran mylodontid *Glossotherium* (Table A1). *Toxodon* values point to a diet based on mixed C_3 – C_4 environments, agreeing with other studies (e.g. MacFadden and Shockey, 1997; MacFadden, 2005; Dantas et al., 2020, 2021). Statistically significant differences have been obtained among taxa as reported through an ANOVA test ($F = 7.275$, $p = 0.001$). According to Tukey's post-hoc analyses (Table A2), *Glossotherium* and *Toxodon* showed significantly higher $\delta^{13}\text{C}$ values than *Equus* and *Megatherium*. The first two genera showed generalist diet (see above comments on *Toxodon*), within intermediate C_3 – C_4 vegetation, while *Equus* values were on the boundary between pure C_3 and mixed C_3 – C_4 environments and *Megatherium* showed a pure C_3 -diet.

Regarding $\delta^{18}\text{O}$ values, *Toxodon* and *Megatherium* showed the lowest value (27.7‰) while *Glossotherium* showed the highest one (30.8‰) (Table A1; Fig. 2). The taxa of Santa Rosa showed statistically significant differences (ANOVA, $F = 4.665$, $p = 0.009$). However, according to Tukey's post-hoc analyses (Table A2), *Toxodon* (lower $\delta^{18}\text{O}$ values) was the only one that showed significant differences with *Glossotherium* and *Hemiauchenia*, suggesting that this notoungulate could have been ingesting water from sources with a lower degree of evaporation.

Playa del Barco's $\delta^{13}\text{C}$ values point to a general preference of all mammalian assemblage for intermediate C_3 – C_4 open vegetation, being *Morenelaphus* the only taxon consuming C_3 plants from wooded areas. This locality showed a minimum value of $\delta^{13}\text{C}$ of -11.4‰ for *Morenelaphus* and a maximum of -2.2‰ for xenarthran mylodontid *Lestodon* (Table A1). $\delta^{13}\text{C}$ – $\delta^{18}\text{O}$ ellipses could not be recovered for *Megatherium*, *Equus* and the xenarthran mylodontid *Scelidotherium*, but they showed similar dietary preferences to those described at Santa Rosa, as did *Toxodon* (Fig. 2). Regarding the gomphoteriid *Stegomastodon*, it consumed an intermediate C_3 – C_4 diet, presenting a wide dietary range as also seen in previous studies (e.g. Sánchez et al., 2004; Domingo et al., 2012). The $\delta^{13}\text{C}$ values of *Morenelaphus* were indicative of a pure C_3 diet. As observed at Cascada del Paleolama, this taxon probably inhabited and consumed food resources from more wooded areas, in contrast to the study of tooth enamel microwear of this taxon which suggests a mixed-feeding diet with significant use of grasses (Rotti et al., 2018). An ANOVA test reported statistically significant differences among taxa ($F = 23.69$, $p < 0.001$). According to Tukey's post-hoc analyses, the two most extreme genera showed significant differences: (1) *Lestodon* (higher $\delta^{13}\text{C}$ values) with *Morenelaphus* and *Stegomastodon*; and (2) *Morenelaphus* (lower $\delta^{13}\text{C}$ values) with *Lestodon*, *Stegomastodon*, and *Toxodon* (Fig. 2, Table A2). Although *Megatherium* and *Scelidotherium* could not be included in the statistical analysis due to the shortage of data points, taking into account the different xenarthran diet-to-enamel

Table 1

Summary of stable isotope values of mammalian fossils from all the localities of the Pampean region analysed in this study (late Pleistocene). Locality, phase, age, taxa, number of carbonate samples (#C), mean and standard deviation (SD) $\delta^{13}\text{C}$ (‰VPDB), $\delta^{18}\text{O}_{\text{CO}_3}$ (‰ VSMOW), number of phosphate samples (#P), mean and standard deviation (SD) $\delta^{18}\text{O}_{\text{PO}_4}$ (‰ VSMOW), mean \pm standard deviation $\%C_4$ diet of equids (Koch et al., 2004), inferred mean MAP (mm/year) (Kohn, 2010) with altitude and latitude correction, and inferred mean MAT (°C) (Dansgaard, 1964; Huertas et al., 1995). Further details of the taxa and total isotopic dataset are available in Table A1.

Locality	Phase	Age	Taxa (Genus)	#C	Mean $\delta^{13}\text{C}$ (‰ VPDB)	SD $\delta^{13}\text{C}$ (‰ VPDB)	Mean $\delta^{18}\text{O}_{\text{CO}_3}$ (‰ VSMOW)	SD $\delta^{18}\text{O}_{\text{CO}_3}$ (‰ VSMOW)	#P	Mean $\delta^{18}\text{O}_{\text{PO}_4}$ (‰ VSMOW)	SD $\delta^{18}\text{O}_{\text{PO}_4}$ (‰ VSMOW)	$\%C_4$ -diet- equids	MAP (mm)	MAT (°C)
Paso Otero	post-LGM	11,628 cal BP ^a	<i>Equus</i>	3	-10.6	0.4	30.3	0.9	1	20.1		11 \pm 3	810	14.9
			<i>Eutatus</i>	1	-11.7		28.2		1	20.5				
			<i>Lama</i>	3	-10.5	0.9	33.3	1.3	2	24.4	0.4			
			<i>Macrauchenia</i>	1	-9.5		29.1		1	21.2				
Arroyo Chasicó	post-LGM	12,673 cal BP ^a	<i>Equus</i>	2	-5.3	0.7	28.8	0.8	2	21.0	1.2	47 \pm 5		16.6
			<i>Macrauchenia</i>	1	-8.8		26.9		1	17.9				
Zanjón Seco	post-LGM	12.8–11.5 cal BP ^a	<i>Equus</i>	4	-10.8	0.5	29.7	0.7	4	20.6	0.6	10 \pm 3	984	15.9
Luján	post-LGM	13,682 cal BP ^a	<i>Equus</i>	2	-11.5	0.4	30.5	0.1	1	21.2		6 \pm 3	1229	17.0
			<i>Hippidion</i>	4	-11.3	0.6	30.5	0.2	3	21.3	0.4			
Arroyo Tapalqué	post-LGM	16,369–8444 cal BP ^a	<i>Equus</i>	2	-8.2	0.4	29.8	0.1	1	21.2		19 \pm 8	480	16.4
			<i>Hippidion</i>	4	-10.1	1.0	30.2	1.2	3	20.8	1.1			
Río Salado	post-LGM	17,281–13,411 cal BP ^a	<i>Hippidion</i>	3	-10.1	1.9	29.1	0.9	3	20.0	0.2	15 \pm 13	785	14.6
Playa del Barco	LGM	19,849 cal BP ^b	<i>Equus</i>	1	-6.7		29.1		0			39		
			<i>Lestodon</i>	7	-3.6	1.6	27.8	0.5	6	18.8	0.5			
			<i>Megatherium</i>	2	-7.1	0.1	28.2	0.1	2	18.7	0.1			
			<i>Morenelaphus</i>	7	-10.2	0.8	29.3	0.4	5	20.7	0.8			
			<i>Scelidotherium</i>	1	-3.9		26.8		1	18.0				
			<i>Stegomastodon</i>	5	-6.3	2.1	29.1	1.0	4	20.7	1.2			
			<i>Toxodon</i>	9	-5.1	1.7	28.2	0.9	6	19.8	1.1			
			<i>Equus</i>	5	-7.9	0.5	29.1	0.4	5	20.0	0.4			
			<i>Glossotherium</i>	4	-4.8	1.8	29.8	0.7	4	20.7	0.6			
			<i>Hemiauchenia</i>	4	-6.9	0.6	29.9	0.2	4	20.9	0.3			
Santa Rosa	LGM	28,170 cal BP ^c	<i>Lama</i>	2	-8.2	0.3	29.8	0.2	2	20.9	0.1	31 \pm 13		14.8
			<i>Megatherium</i>	5	-7.6	0.8	28.6	0.8	5	19.6	0.9			
			<i>Scelidotherium</i>	1	-3.2		29.7		1	20.8				
			<i>Toxodon</i>	5	-5.5	1.3	28.5	0.8	5	19.5	0.9			
			<i>Equus</i>	13	-7.4	2.1	29.9	1.0	11	20.6	1.0			
			<i>Hemiauchenia</i>	5	-8.0	0.7	28.9	0.4	5	20.0	0.3			
			<i>Hippidion</i>	2	-8.4	0.4	29.5	0.6	2	20.7	0.7			
			<i>Lama</i>	1	-9.0		32.6		1	23.4				
			<i>Macrauchenia</i>	2	-6.7	1.4	28.9	1.0	2	19.8	1.1			
			<i>Morenelaphus</i>	1	-9.8		29.5		1	20.4				
Cascada del Paleolama	LIG	Unpublished data (MIS 5e, ~128,000–116,000 cal BP years ^d)	<i>Toxodon</i>	4	-7.9	0.3	29.7	0.3	4	20.8	0.4	30 \pm 13		15.9

^a Prado et al. (2015).

^b Tomassini et al. (2020).

^c Montalvo et al. (2013).

^d Stirling et al. (1998).

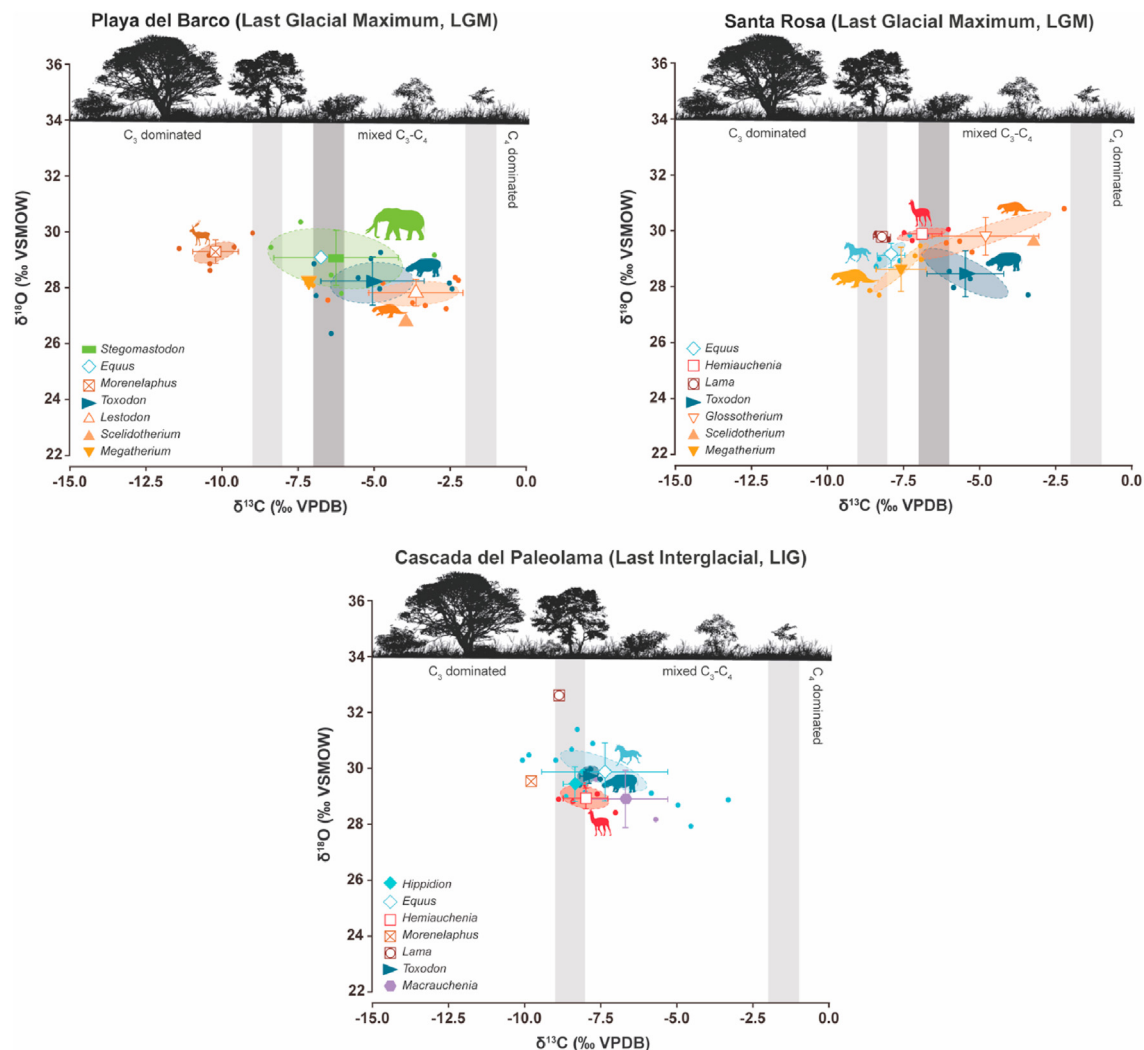


Fig. 2. Raw and mean (± 1 standard deviation) $\delta^{13}\text{C}$ (‰ VPDB) and $\delta^{18}\text{O}$ (‰ VSMOW) values for different mammals from Playa del Barco (LGM), Santa Rosa (LGM) and Cascada del Paleolama (LIG). Taxon silhouettes indicate taxa for which standard ellipse areas (SEAs) generated by SIBER, representing isotopic niches, could be calculated. The grey vertical bars depict the vegetation $\delta^{13}\text{C}$ cut-off values between a C_3 -dominated diet, an intermediate C_3 – C_4 diet, and a C_4 -dominated diet. The lightest grey denotes a $\delta^{13}\text{C}$ bioapatite-diet enrichment of +14.1‰ (Cerling and Harris, 1999), whereas the darkest one corresponds to an enrichment of +15.6‰ for xenarthrans (Tejada-Lara et al. 2009).

$\delta^{13}\text{C}$ fractionation, the former had an C_3 dominated diet similar to *Morenelaphus*, while the latter showed a mixed C_3 – C_4 diet close to *Lestodon* (Fig. 2).

Regarding $\delta^{18}\text{O}$ values, *Toxodon* showed the lowest value (26.4‰) and *Stegomastodon* showed the highest one (30.4‰) (Table A1; Fig. 2). Statistical significant differences among taxa have been obtained as reported through an ANOVA test ($F = 6.352$, $p = 0.003$). According to Tukey's post-hoc analyses, *Lestodon* showed significant lower $\delta^{18}\text{O}$ values than *Morenelaphus* and *Stegomastodon*; and *Morenelaphus* showed significant higher $\delta^{18}\text{O}$ values than *Lestodon* and *Toxodon* (Table A2). This may suggest that *Lestodon* consumed water from water sources with a lower degree of evaporation. Nevertheless, since *Morenelaphus* is not an obligate drinker its $\delta^{18}\text{O}$ values do not reliably represent the isotopic composition of meteoric water. Thus, climatic and/or hydrological information cannot be extracted from this taxa.

Environmental changes are related to glacial and interglacial phases (Cione et al., 2015). The Pleistocene experienced a reduction of subtropical and tropical biomes, resulting in the expansion of open biomes, related to glacial periods (Ortiz-Jaureguizar and

Cladera, 2006). We interpreted that this occurred in Santa Rosa and Playa del Barco during the LGM since our results indicate that these localities experienced more open and arid conditions than Cascada del Paleolama (LIG). Statistical significant differences in carbon and oxygen isotopes were found between *Toxodon* from Cascada del Paleolama and Playa del Barco, and *Hemiauchenia* from Cascada del Paleolama and Santa Rosa (Table A3). Both taxa presented higher $\delta^{13}\text{C}$ values during the LGM, indicative of a more open environment associated with higher aridity, and lower $\delta^{18}\text{O}$, possibly due to lower temperature and/or more continental conditions related to the sea level drop during glacial periods.

3.2. Palaeoclimatic evaluation through late Pleistocene

Last Interglacial (LIG). It includes the locality of Cascada del Paleolama. The genus of equid analysed in this phase is *Equus*. Although its tooth enamel $\delta^{13}\text{C}$ values point to a flexible diet with a preference for mixed C_3 – C_4 plant resources, some individuals also presented a pure C_3 vegetation diet (Fig. 3). Due to the consumption of a relatively high percentage of C_4 plants ($30 \pm 13\%$; Table 1, Fig. 3),

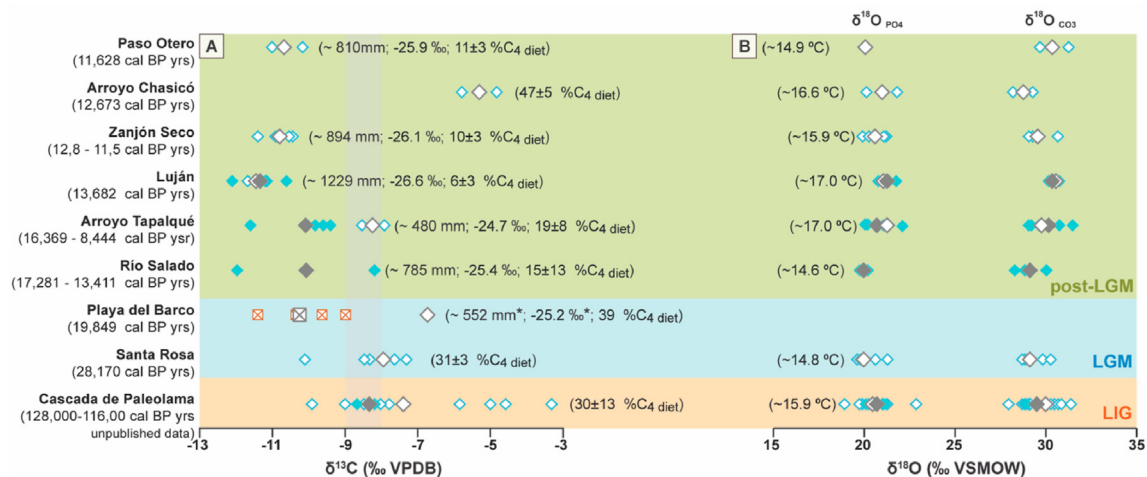


Fig. 3. Equid and cervid isotopic values from the studied sites. A) Raw and mean tooth enamel $\delta^{13}\text{C}$ values (‰ VPDB) of *Equus* (empty diamonds), *Hippidion* (solid diamonds) and *Morenelaphus* (squares with crosses, *). Estimated Mean Annual Precipitation values (mm), calculated mean values of the modern equivalent of diet composition ($\delta^{13}\text{C}_{\text{diet, meq}}$, ‰ VPDB) and estimated values of the percentage of C_4 plants in the equid diet are shown in brackets. B) Raw and mean tooth enamel $\delta^{18}\text{O}_{\text{PO}_4}$ and $\delta^{18}\text{O}_{\text{CO}_3}$ values (‰ VSMOW) of *Equus* and *Hippidion*. Estimated Mean Annual Temperature ($^{\circ}\text{C}$) values are shown. MAP values are not presented for Arroyo Chasicó, Santa Rosa and Cascada del Paleolama because the model of Kohn et al. (2004) may not work for diets with a significant component of C_4 vegetation in herbivore diets. The different background colours refer to the three studied phases: Last Interglacial period (LIG, orange), Last Glacial Maximum (LGM, blue), post-Last Glacial Maximum (post-LGM, green).

it was not possible to calculate the mean annual precipitation following Kohn (2010)'s study. Based on *Equus* $\delta^{18}\text{O}_{\text{PO}_4}$ values, a MAT of 15.9 $^{\circ}\text{C}$ was calculated (Table 1, Fig. 3). Due to the lack of MAP values, it was not possible to classify the biome according to Whittaker's biome classification (Whittaker, 1962).

Last Glacial Maximum (LGM). It corresponds to the localities of Santa Rosa and Playa del Barco. The percentage of C_4 plants in the diet of *Equus* from both sites ranges from $31 \pm 3\%$ – 39% , the highest percentages after the Arroyo Chasicó site (post-LGM). These values point to a preference for consumption of mixed C_3 – C_4 plant resources. As in the case of LIG, the MAP cannot be calculated based on this taxon. However, the values for *Morenelaphus* in Playa del Barco correspond to a diet based on pure C_3 plants and a MAP of 552 mm has been estimated for this site (Table 1, Fig. 3).

The MAT calculated from the $\delta^{18}\text{O}_{\text{PO}_4}$ values of Santa Rosa's *Equus* is 14.8 $^{\circ}\text{C}$ (Table 1, Fig. 3), one of the lowest values found in the studied localities. The MAT value for the Playa del Barco fossil site could not be worked out as *Morenelaphus* is not considered an obligate drinker and, therefore, its $\delta^{18}\text{O}$ is not representative of the water drunk. Thus, the biome that may have existed for this phase was estimated from the MAP calculated at Playa del Barco and the MAT at Santa Rosa. It would correspond to a woodland/shrubland domain near the boundary with temperate grasslands (Fig. 4).

Post-Last Glacial Maximum (post-LGM). It includes several localities of the Buenos Aires Province (see Fig. 1). The $\delta^{13}\text{C}$ values of *Equus* and *Hippidion* point to consumption of plants from mostly C_3 environments, with C_4 plants in the diet ranging from 6 ± 3 to $19 \pm 8\%$ (Table 1, Fig. 3), except for the Arroyo Chasicó site where *Equus* shows the highest $\delta^{13}\text{C}$ values. The results for this site point to a mixed C_3 – C_4 diet, with the highest percentage of C_4 plants being $47 \pm 5\%$ (Table 1, Fig. 3) and therefore, as mentioned above, MAP could not be calculated following Kohn (2010)'s study. The estimated MAP values for the other fossil sites in the post-LGM phase range from 480 to 1229 mm (Table 1, Fig. 3), while MAT ranges from 14.6 to 17 $^{\circ}\text{C}$. The climate inferred for this phase would be mostly related to woodland/shrubland landscapes, although some localities also point to temperate seasonal forests and

temperate grasslands (Fig. 4). This variability might suggest a mosaic-type biome in the region, and/or humid (temperate seasonal forests) or arid (temperate grasslands) stages during the post-LGM period, such as the Bølling/Allerød (15–14.6 yrs BP; Weaver et al., 2003; Royer and Finney, 2020) or the Younger Dryas (12.9–11.7 yrs BP; Rasmussen et al., 2006; Cheng et al., 2020), respectively. The lack of accurate dating of the materials from the fossil sites of this phase (Table 1) does not allow us to correlate the different peaks with our localities. Nevertheless, Arroyo Chasicó (12,673 cal BP yrs, Table 1) points to the more arid conditions of this phase, which can be justified by correlating this site with cold/dry event Younger Dryas (Prado et al., 2015).

3.3. Relevance of C_4 vegetation during the LGM

C_4 plants are important components in temperate and arid grasslands and tropical savannas (Strömberg, 2011). Although C_4 vegetation is more successful in latitudes with relatively warm temperatures, abundant summer rainfall and adequate insolation, these plants can cope with tough conditions implying water stress, some degree of salinity in the soil and low atmospheric CO_2 levels (Sage et al., 1999; Tiplle and Pagani, 2007; Edwards and Smith, 2010), which may have benefited them during Pleistocene glacial periods (Collatz et al., 1998). Their $\delta^{13}\text{C}$ range is more restricted than that of C_3 plants (Cerling et al., 1997), but their isotopic values are more similar to those of the atmosphere due to their more efficient CO_2 fixation (Koch et al., 2004). The quantum yield (carbon gain per absorbed photon) of C_3 plants decreases with increasing temperature as photorespiration rates increase, whereas in C_4 plants they remain low or unchanged (Ehleringer et al., 1997; Koch, 1998). Thus, C_3 plants dominate when the growing season is cool. Considering that cooler temperatures are recorded during the LGM around the world, it would be expected that C_3 plants would dominate in the Pampean region during this phase. However, our data suggest more open environments during the LGM in the study area. For example, the percentage of C_4 plants in the equids diet is 31 ± 3 – 39% compared to post-LGM values $6 \pm 3\%$ to $19 \pm 8\%$ (except

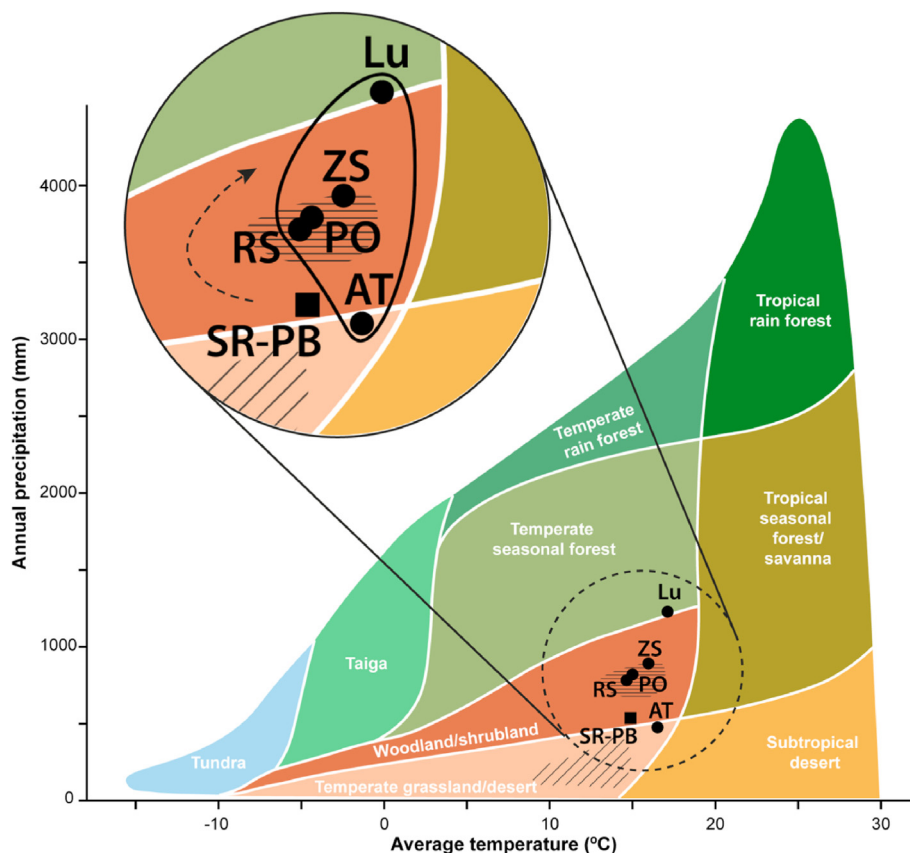


Fig. 4. Whittaker's biome classification diagram showing the different terrestrial biomes as a function of current Mean Annual Precipitation (MAP, in mm) and Mean Annual Temperature (MAT, in °C). The fossil sites studied are represented according to their MAP and MAT values calculated from the isotopic values of the equids *Equus* and *Hippidion*, and the cervid *Morenelaphus*. The square represents the Last Glacial Maximum and the circles the post-Last Glacial Maximum. The area with diagonal lines represents the modern climate in the north-eastern Patagonia, and the area with horizontal lines represents the current Pampean region climate. In the zoomed region the fossil sites of post-LGM are enclosed in an area delimited by a black line and the arrows indicate the evolution of the climate. Arroyo Chasicó and Cascada del Paleolama are not plotted because MAP values are not available. Santa Rosa and Playa del Barco are depicted together because each site contributes a variable (MAP and MAT, respectively). For the name of the fossil localities see figure caption 1. Graph modified from Whittaker (1975).

Arroyo Chasicó, $47 \pm 5\%$) (Fig. 4). Statistical analyses showed significant differences (Table A3) in $\delta^{13}\text{C}$ values between: (1) *Equus* of Zanjón Seco and Paso Otero (pure C_3 diet) with Cascada del Paleolama (mixed C_3 – C_4); (2) *Toxodon* of Cascada del Paleolama (lowest $\delta^{13}\text{C}$ values) with Playa del Barco (highest $\delta^{13}\text{C}$ values); and (3) *Hemiauchenia* of Cascada del Paleolama (lower $\delta^{13}\text{C}$ values) with Santa Rosa.

It is important to note that some taxa could not be included in these analyses due to lack of sample, such as: *Hippidion* (LIG and post-LGM), *Macrauchenia* (LIG and post-LGM) and *Lama* (LIG, LGM and post-LGM). During the post-LGM phase, *Macrauchenia* values are indicative of a pure C_3 diet, nevertheless, during LIG it shows a mixed C_3 – C_4 diet (Fig. 5). During the LIG and the post-LGM *Lama* shows a mostly C_3 diet, however, during the LGM it incorporates more C_4 plants. Overall, the faunal communities of the LGM localities show mixed C_3 – C_4 diets except for *Megatherium* and *Morenelaphus* (discussed in section 3.1), while in the post-LGM they are diets based on mostly C_3 plants (Fig. 5). The interglacial phase displays an intermediate situation, configured by more open vegetation than during the post-LGM, but not as much as the open environments from the LGM.

Bioapatite $\delta^{13}\text{C}$ values from all the considered taxa suggest that during the LGM in the Pampean region there was a higher incorporation of C_4 plants food resources, which may reflect a relatively higher abundance of C_4 vegetation compared to C_3 plants. Although, this is not expected for cold conditions of a glacial period.

Nevertheless, we must consider that the quantum yield of C_3 plants is also affected by the decrease in the atmospheric CO_2 pressure ($\text{pCO}_{2\text{atm}}$), a factor that does not significantly affect C_4 plants (Ehleringer et al., 1997). During interglacial periods, $\text{pCO}_{2\text{atm}}$ values above 280 ppmv are inferred, whereas for glacial periods these values decrease to 180 ppmv (Siegenthaler, 2005; Lüthi et al., 2008). Specifically, $\text{pCO}_{2\text{atm}}$ values for the studied phases are: LIG, 273 ppmv (Otto-Bliesner et al., 2013), LGM, 200 ppmv (Cowling et al., 2004), and post-LGM, 235 ppmv (Koch et al., 2004). The low $\text{pCO}_{2\text{atm}}$ values recorded during the LGM (Fig. 5) favoured the dominance of C_4 plants despite low temperatures (Cerling et al., 1998; Harrison and Prentice, 2003; Woillez et al., 2011; McGee, 2020).

Nevertheless, low $\text{pCO}_{2\text{atm}}$ is not sufficient to drive the expansion of C_4 plants if other factors are unfavourable (Huang et al., 2001). The dominance of C_4 plants may have been driven by the combined effects of low $\text{pCO}_{2\text{atm}}$ and an increase in aridity. Aridification during the LGM may have been due to increased continentality in the Pampean region caused by the 140 m sea level drop and changes in ocean currents (Tonello and Prieto, 2008; Ponce et al., 2011; Gasparini et al., 2016). Our results support this scenario, as during the LGM one of the lowest MAP values is recorded from bioapatite $\delta^{13}\text{C}$ values (Fig. 3). In addition, our results show slightly lower $\delta^{18}\text{O}$ values in the LGM localities compared to the other two phases (Fig. 5). No significant differences were found between $\delta^{18}\text{O}$ values, except those mentioned in section 3.1

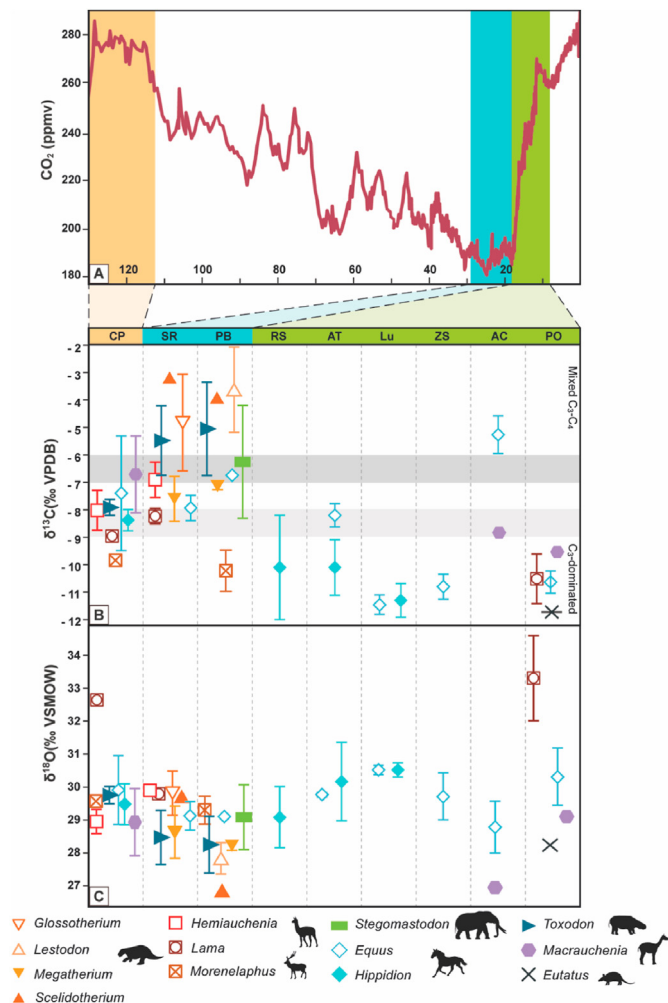


Fig. 5. A) Composite reconstructions of atmospheric carbon dioxide from Bereiter et al. (2015). The orange bar corresponds to the Last Interglacial (LIG), the blue bar to the Last Glacial Maximum (LGM) and the green bar to the post-LGM glacial period; B) $\delta^{13}\text{C}$ (‰ VPDB) values and C) $\delta^{18}\text{O}$ (‰ VSMOW) mean ± 1 standard deviation values of all the mammals from the selected fossil sites. For the name of the fossil localities see figure caption 1. The grey horizontal bars depict the vegetation $\delta^{13}\text{C}$ cut-off values between a C₃-dominated diet and an intermediate C₃-C₄ diet. The lightest grey denotes a $\delta^{13}\text{C}$ bioapatite-diet enrichment of +14.1‰ (Cerling and Harris, 1999), whereas the darkest one corresponds to an enrichment of +15.6‰ for xenarthrans (Tejada-Lara et al. 2009).

between the LIG and LGM (*Toxodon* and *Hemiauchenia*), but it must be taken into account that some taxa were not included in the statistical analysis, such as *Lama*, which presents the highest $\delta^{18}\text{O}$ values for the LIG and the post-LGM and lower values for the LGM (Fig. 5). These lower $\delta^{18}\text{O}$ values may be consequence of an increase in aridity and continentality during the LGM, which results in enrichment of the light isotopes of the water masses due to less evaporation and greater distance from the sea. Under these conditions (aridity, continentality, low $p\text{CO}_2\text{atm}$), C₄ plants may have dominated in the Pampean region during the LGM as also occurred in other parts of South America (e.g. Novello et al., 2019).

3.4. Variations in atmospheric circulation in association to climate changes in the Pampean region

The changes identified in environmental and climatic variables among the three phases might be related to the increase of continentality associated to water retention in polar ice sheets and the

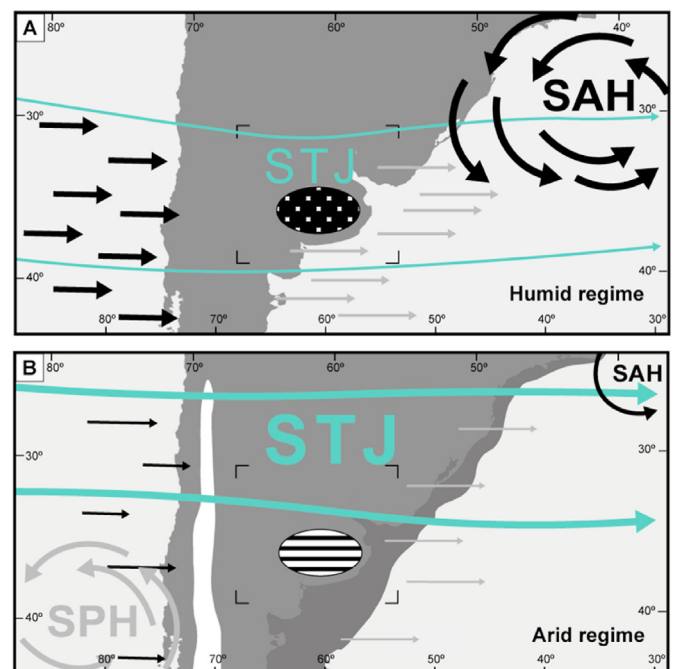


Fig. 6. Scenarios of atmospheric circulation in the Pampean region of Argentina during the two proposed climatic regimes in the study area: A) humid-temperate regime, mottled areas, B) arid-temperate regime, striped areas. The maps show the sea-level corresponding to both the humid (+6m) and arid regime (−140m) (see Ponce et al., 2011; Gowan et al., 2021). STJ, approximate path of the Subtropical Jet Stream. SAH, South Atlantic High; SPH, South Pacific High. Arrows indicate main winds: grey, dry winds; black, humid winds; blue, STJ path. The thickness of the blue arrows is proportional to their strength; the black arrows are proportional to their strength and water carrying capacity. The atmospheric circulation reconstruction is based on Iriondo and García (1993), Tonni et al. (1999), Gallego et al. (2005) and Gili et al. (2017).

resulting sea-level lowering (Rabassa et al., 2005), and the variations in atmospheric CO₂, which appear to be mostly connected to shifts in the strength and efficiency of the ocean biological carbon pump (Sigman and Boyle, 2000; Kohfeld and Ridgwell, 2009; d'Orgeville et al., 2010; Yu et al., 2014). Furthermore, these changes might be largely controlled by alterations in atmospheric circulation.

All these processes were related to the glacial-interglacial alternation, which was in turn regulated by the variations in Earth's energy balance associated to the Milankovitch cycles (Ravibhanu et al., 2020; see Caccamo and Magazù, 2021 and references therein). Therefore, we used information derived from atmospheric circulation models (Gallego et al., 2005; Garreaud et al., 2009; Marengo et al., 2012) as a key to propose possible scenarios that would explain the observed climatic variability in the Pampean region during the late Pleistocene (Fig. 6).

The Pampean region is currently affected by mid-latitude westerly winds that extend through the upper troposphere reaching a maximum speed in what is known as the "Subtropical Jet Stream" (STJ) (Gallego et al., 2005; Garreaud et al., 2009). Winds and precipitation are also influenced by the high-pressure systems and the anticyclonic circulation of the South Atlantic (SAH) and South Pacific (SPH) oceans (Iriondo and García, 1993; Prieto, 1996). The SAH introduces warm and humid air masses from the north/northeast into de Pampas, while the SPH introduces cold and dry winds from the south/southwest. Latitudinal shifts of the STJ, the high-pressure systems and westerly winds, are evidenced by changes in regional precipitation patterns (Romero et al., 2021). Our isotopic values allowed us to infer a low MAT difference ($\pm 3.6^\circ\text{C}$) and a higher MAP variation (± 677 mm) during the lapse of

the late Pleistocene. From our results, together with current atmospheric circulation models, we have identified two possible climate scenarios in this region: a humid regime (during the Last Interglacial) and an arid regime (during the Last Glacial Maximum) (Fig. 6).

During the arid climatic regime, the STJ was strong but moved northward towards latitudes around 30°S (Prieto, 1996; Gallego et al., 2005; Garreaud et al., 2009; Gili et al., 2017) and no longer affected the Pampean region. In addition, the westerlies as well as the SAH winds that transport humidity were weakened and had less influence in the region (Iriondo and García, 1993; Garreaud et al., 2009). On the other hand, there was an increase in SPH strength, which made cold and dry winds more important in the studied area (Rabassa et al., 2005). Our $\delta^{13}\text{C}$ and $\delta^{18}\text{O}$ isotopic values during the LGM support this climatic scenario. One of the lowest MAP (552 mm) and MAT (14.8 °C) values is recorded during this phase (Fig. 3). Taxa from Santa Rosa and Playa del Barco show higher $\delta^{13}\text{C}$ values than the other phases, indicating an increased consumption of C_4 plants in the diet of these taxa. In addition, $\delta^{18}\text{O}$ values are slightly lower than in the other study phases. Both results are justified by an increase in aridity and continentality (see discussion section 3.3). As a consequence of the coastline shift, the Brazil and Malvinas currents moved to the north and east, respectively; modifying the Pampean winter storm pattern, intensifying continentality and increasing water deficit in the area (Rabassa et al., 2005). Therefore, during this lapse, a dry-temperate regime was installed in the area, similar to the one currently present in northeastern Patagonia (Fig. 6). This has already been seen in other studies, which show that most of the Pampean region had a colder and drier climate than the present (Tonni et al., 1999; Tonello and Prieto, 2010; Berman et al., 2016). Quattrocchio et al. (2008) suggested arid environmental conditions for the southwestern Buenos Aires province, with sporadic precipitations during the late Pleistocene, based on the study of different pollen assemblages and ostracod associations in the area (Quattrocchio et al., 2008). Mammalian studies also report similar conditions, with the Pampean region inhabited by fauna typical of open habitats, arid to semi-arid, during the LGM (Cione et al., 2015).

During the humid climatic regime, a weakened STJ was over the Pampean region (Gallego et al., 2005). Although the westerly winds had a higher capacity for carrying humidity, due to the higher temperatures, this humidity was retained in the western slopes of the Andes. On the contrary, the SAH had a strong influence (Iriondo and García, 1993; Garreaud et al., 2009), bringing warm and humid air masses to the Pampean region. Our LIG isotopic values allow us to infer a MAT of 15.9 °C (Fig. 3), although MAP values could not be calculated. The taxa show $\delta^{13}\text{C}$ values that indicate diets preferably based on C_3 plants but also in mixed C_3 – C_4 environments. Therefore, it can be interpreted that the environments during this phase are less arid than during the LGM and are better adjusted to this climatic regime. Regarding the post-LGM values, most fossil sites fit this climatic regime with high MAP and MAT values and low percentages of C_4 plants in the diet of the taxa (Fig. 3), indicating less arid environments. In fact, the current climatic conditions in the Pampean region are very close to the ones shown in this phase (Fig. 4). However, it should be considered, that this phase experienced a wide climatic variability (Fig. 3), and there are localities more aligned with the arid regime, such as Arroyo Chasicó, which could be related with the Younger Dryas event (Prado et al., 2015).

4. Conclusions

This work provides new insights on the palaeoecology, palaeoenvironment, and palaeoclimate during late Pleistocene glacial-interglacial cycles of the late Pleistocene in southern South

America by means of $\delta^{13}\text{C}$ and $\delta^{18}\text{O}$ isotopic analysis on mammalian bioapatite. The study of temporal sequences in the same geographical area facilitates the analysis of variability in parameters such as temperature, precipitation, and cover vegetation. Our results show that Pampean mammals occupied a range of habitats from woodlands/open C_3 grassland to mixed C_3 – C_4 grassland. During the Last Glacial Maximum, taxa show a higher consumption of C_4 plants, whereas during the post-Last Glacial Maximum phase isotopic values point to diets based on pure C_3 environments. In the Last Interglacial, taxa show intermediate diets based on C_3 and mixed C_3 – C_4 vegetation sources. The higher consumption of C_4 plants during the LGM might be related to a reduction of forested areas conditioned by a combination of environmental and climatic factors during the glacial phase, such as a lower pCO_2atm and an increase in aridity.

$\delta^{13}\text{C}$ values allowed us to infer a higher Mean Annual Precipitation during the post-LGM phase (480–1229 mm) compared to the LGM (552 mm). In addition, we inferred, from the $\delta^{18}\text{O}$ values, an extremely reduced temperature variation (± 3.6 °C) from the LIG to the post-LGM phases. We interpret that the global conditions during the glacial-interglacial episodes influenced the displacement of the oceanic anticyclonic centres, both in the Pacific and the Atlantic, controlling the climate in the Pampean region. Our results point to a humid climatic regime in the area during the Last Interglacial, partly conditioned by the strong influence of the SAH, and an arid regime for the Last Glacial Maximum. We observed a wide climatic variation in the post-LGM phase that may be associated with post-glacial climatic oscillations. Finally, this study demonstrates that there was a greater variation in precipitation and aridity than in temperature in the Pampean region throughout the late Pleistocene interglacial-glacial phases.

Authors' contributions

Dánae Sanz-Pérez: Conceptualization; Formal analysis; Investigation; Project administration; Visualization; Writing – original draft; **Manuel Hernández Fernández:** Conceptualization; Project administration; Investigation; Supervision; Visualization; Writing – original draft; **Rodrigo L. Tomassini:** Conceptualization; Funding acquisition; Project administration; Resources; Supervision; Visualization; Writing – original draft; **Claudia Montalvo:** Funding acquisition; Resources; Supervision; Writing – review & editing; **Germán M. Gasparini:** Resources; Writing – review & editing; **Elisa Beilinson:** Resources; Writing – review & editing; **Laura Domingo:** Conceptualization; Funding acquisition; Project administration; Investigation; Resources; Supervision; Visualization; Writing – original draft.

Declaration of competing interest

The authors declare that they have no known competing financial interests or personal relationships that could have appeared to influence the work reported in this paper.

Acknowledgements

This work was supported by the Ministerio de Ciencia e Innovación (Project PGC 2018-094955-A-I00); National Geographic-Waitt Foundation grant #W467-16; the Facultad de Ciencias Exactas y Naturales, Universidad Nacional de La Pampa (G13 Grant); the Secretaría de Ciencia y Tecnología of the Universidad Nacional del Sur (PGI 24 H/154); DSP have a predoctoral grant funded by the Ministerio de Ciencia, Innovación y Universidades (PRE 2019-089848). DSP, MHF and LD acknowledge the research group UCM 910607 on Evolution of Cenozoic Mammals

and Continental Palaeoenvironments. We are indebted to M. Reguero (Museo de La Plata), N. Sánchez (Museo Municipal de Ciencias Naturales Vicente Di Martino), and R. Caputo (Museo Municipal de Ciencias Naturales Carlos Darwin) for enabling collection access. We acknowledge J.L. Prado (UNICEN) for the sampling of some Pleistocene samples. We thank P.L. Koch (University of California Santa Cruz) for access to his laboratory and D. Andreasen (UCSC) for assistance with stable isotope analysis. Thanks are also extended to D. Schreve and two anonymous reviewers, whose comments and suggestions greatly improved this paper.

Appendix A. Supplementary data

Supplementary data to this article can be found online at <https://doi.org/10.1016/j.quascirev.2022.107555>.

References

- Antoine, P., Rousseau, D.-D., Degeai, J.-P., Moine, O., Lacroix, F., Kreutzer, S., Fuchs, M., Hatté, C., Gauthier, C., Svoboda, J., Lisá, L., 2013. High-resolution record of the environmental response to climatic variations during the Last Interglacial–Glacial cycle in Central Europe: the loess-palaeosol sequence of Dolní Věstonice (Czech Republic). *Quat. Sci. Rev.* 67, 17–38. <https://doi.org/10.1016/j.quascirev.2013.01.014>.
- Araguás-Araguás, L., Froehlich, K., Rozanski, K., 2000. Deuterium and oxygen-18 isotope composition of precipitation and atmospheric moisture. *Hydrol. Process.* 14, 1341–1355. [https://doi.org/10.1002/1099-1085\(20000615\)14:8<1341::AID-HYP983>3.0.CO;2-Z](https://doi.org/10.1002/1099-1085(20000615)14:8<1341::AID-HYP983>3.0.CO;2-Z).
- Beck, H.E., Zimmermann, N.E., McVicar, T.R., Vergopolan, N., Berg, A., Wood, E.F., 2018. Present and future Köppen-Geiger climate classification maps at 1-km resolution. *Sci. Data* 5, 180214. <https://doi.org/10.1038/sdata.2018.214>.
- Bereiter, B., Eggelston, S., Schmitt, J., Nehrbass-Ahles, C., Stocker, T.F., Fischer, H., Kipfstuhl, S., Chappellaz, J., 2015. Revision of the EPICA Dome C CO₂ record from 800 to 600 kyr before present. *Geophys. Res. Lett.* 42, 542–549. <https://doi.org/10.1002/2014GL061957>.
- Berman, A.L., Silvestri, G.E., Tonello, M.S., 2016. Differences between last glacial maximum and present-day temperature and precipitation in southern South America. *Quat. Sci. Rev.* 150, 221–233. <https://doi.org/10.1016/j.quascirev.2016.08.025>.
- Bocherens, H., Cotte, M., Bonini, R., Scian, D., Straccia, P., Soibelzon, L., Prevosti, F.J., 2016. Paleobiology of sabretooth cat *Smilodon populator* in the pampean region (Buenos Aires province, Argentina) around the last glacial maximum: insights from carbon and nitrogen stable isotopes in bone collagen. *Palaeogeogr. Palaeoclimatol. Palaeoecol.* 449, 463–474. <https://doi.org/10.1016/j.palaeo.2016.02.017>.
- Caccamo, M.T., Magazù, S., 2021. On the breaking of the Milankovitch cycles triggered by temperature increase: the stochastic resonance response. *Climate* 9, 67. <https://doi.org/10.3390/cli9040067>.
- Cerling, T.E., Ehleringer, J.R., Harris, J.M., 1998. Carbon dioxide starvation, the development of C₄ ecosystems, and mammalian evolution. *Philos. Trans. R. Soc. Lond. B Biol. Sci.* 353, 159–171. <https://doi.org/10.1098/rstb.1998.0198>.
- Cerling, T.E., Harris, J.M., 1999. Carbon isotope fractionation between diet and bioapatite in ungulate mammals and implications for ecological and paleoecological studies. *Oecologia* 120, 347–363. <https://doi.org/10.1007/s004420050868>.
- Cerling, T.E., Harris, J.M., MacFadden, B.J., Leakey, M.G., Quade, J., Eisenmann, V., Ehleringer, J.R., 1997. Global vegetation change through the Miocene/Pliocene boundary. *Nature* 389, 153–158. <https://doi.org/10.1038/38229>.
- Cheng, H., Zhang, H., Spötl, C., Baker, J., Sinha, A., Li, H., Bartolomé, M., Moreno, A., Kathayat, G., Zhao, J., Dong, X., Li, Y., Ning, Y., Jia, X., Zong, B., Ait Brahimi, Y., Pérez-Mejías, C., Cai, Y., Novello, V.F., Cruz, F.W., Severinghaus, J.P., An, Z., Edwards, R.L., 2020. Timing and structure of the Younger Dryas event and its underlying climate dynamics. *Proc. Natl. Acad. Sci. United States Am.* 117, 23408–23417. <https://doi.org/10.1073/pnas.2007869117>.
- Cione, A.L., Gasparini, G.M., Soibelzon, E., Soibelzon, L.H., Tonni, E.P., 2015. The Great American Biotic Interchange. *Springer Briefs in Earth System Sciences*. Springer Netherlands, Dordrecht. <https://doi.org/10.1007/978-94-017-9792-4>.
- Clementz, M.T., Fox-Dobbs, K., Wheatley, P.V., Koch, P.L., Doak, D.F., 2009. Revisiting old bones: coupled carbon isotope analysis of bioapatite and collagen as an ecological and palaeoecological tool. *Geol. J.* 44, 605–620. <https://doi.org/10.1002/gj.1173>.
- Collatz, G.J., Berry, J.A., Clark, J.S., 1998. Effects of climate and atmospheric CO₂ partial pressure on the global distribution of C₄ grasses: present, past, and future. *Oecologia* 114, 441–454. <https://doi.org/10.1007/s004420050468>.
- Cowling, S.A., Betts, R.A., Cox, P.M., Ettwein, V.J., Jones, C.D., Maslin, M.A., Spall, S.A., 2004. Contrasting simulated past and future responses of the Amazonian forest to atmospheric change. *Philos. Trans. R. Soc. Lond. B Biol. Sci.* 359, 539–547. <https://doi.org/10.1098/rstb.2003.1427>.
- d'Orgeville, M., Sijp, W.P., England, M.H., Meissner, K.J., 2010. On the control of glacial-interglacial atmospheric CO₂ variations by the Southern Hemisphere westerlies: westerlies and CO₂ variations. *Geophys. Res. Lett.* 37. <https://doi.org/10.1029/2010GL045261> n/a-n/a.
- Dansgaard, W., 1964. Stable isotopes in precipitation. *Tellus* 16, 436–468. <https://doi.org/10.1111/j.2153-3490.1964.tb00181.x>.
- Dantas, M.A.T., Cherkinsky, A., Lessa, C.M.B., Santos, L.V., Cozzuol, M.A., Omena, É.C., Silva, J.L.L. da, Sial, A.N., Bocherens, H., 2020. Isotopic paleoecology ($\delta^{13}\text{C}$, $\delta^{18}\text{O}$) of a late Pleistocene vertebrate community from the Brazilian Intertropical Region. *Rev. Bras. Palaontol.* 23, 138–152. <https://doi.org/10.4072/rbp.2020.2.05>.
- Dantas, M.A., Vieira de Araujo, A., Silva, L.A., Cherkinsky, A., 2021. An isotopic study ($\delta^{13}\text{C}$, $\delta^{18}\text{O}$) of *Panthera onca* (Linnaeus, 1758) from the late Pleistocene of Brazilian Intertropical Region: habitat, isotopic diet composition, and isotopic niche overlap with extinct faunivores. *J. South Am. Earth Sci.* 103666. <https://doi.org/10.1016/j.jsames.2021.103666>.
- de Oliveira, K., Asevedo, L., Calegari, M.R., Gelfo, J.N., Mothé, D., Avilla, L., 2021. From oral pathology to feeding ecology: the first dental calculus paleodiet study of a South American native megamammal. *J. South Am. Earth Sci.* 109, 103281. <https://doi.org/10.1016/j.jsames.2021.103281>.
- Domingo, L., Prado, J.L., Alberdi, M.T., 2012. The effect of paleoecology and paleobiogeography on stable isotopes of Quaternary mammals from South America. *Quat. Sci. Rev.* 55, 103–113. <https://doi.org/10.1016/j.quascirev.2012.08.017>.
- Domingo, L., Koch, P.L., Hernández Fernández, M., Fox, D.L., Domingo, M.S., Alberdi, M.T., 2013. Late neogene and early quaternary paleoenvironmental and paleoclimatic conditions in southwestern Europe: isotopic analyses on mammalian taxa. *PLoS One* 8, e63739. <https://doi.org/10.1371/journal.pone.0063739>.
- Domingo, L., Domingo, M.S., Koch, P.L., Morales, J., Alberdi, M.T., 2017. Carnivorous resource and habitat use in the context of a Late Miocene faunal turnover episode. *Palaeontology* 60, 461–483. <https://doi.org/10.1111/pala.12296>.
- Domingo, L., Tomassini, R.L., Montalvo, C.I., Sanz-Pérez, D., Alberdi, M.T., 2020. The Great American Biotic Interchange revisited: a new perspective from the stable isotope record of Argentine Pampas fossil mammals. *Sci. Rep.* 10, 1608. <https://doi.org/10.1038/s41598-020-58575-6>.
- Edwards, E.J., Smith, S.A., 2010. Phylogenetic analyses reveal the shady history of C₄ grasses. *Proc. Natl. Acad. Sci. United States Am.* 107, 2532–2537. <https://doi.org/10.1073/pnas.0909672107>.
- Ehleringer, J.R., Cerling, T.E., Helliker, B.R., 1997. C₄ photosynthesis, atmospheric CO₂, and climate. *Oecologia* 112, 285–299. <https://doi.org/10.1007/s004420050311>.
- Farquhar, G.D., Ehleringer, J.R., Hubick, K.T., 1989. Carbon isotope discrimination and photosynthesis. *Annu. Rev. Plant Biol.* 40 (1), 503–537. <https://doi.org/10.1146/annurev.pp.40.060189.002443>.
- Gallego, D., Ribera, P., García-Herrera, R., Hernandez, E., Gimeno, L., 2005. A new look for the Southern Hemisphere jet stream. *Clim. Dynam.* 24, 607–621. <https://doi.org/10.1007/s00382-005-0006-7>.
- García-Morato, S., Fernández-Jalvo, Y., Montalvo, C.I., Andrews, P., Marín-Monfort, M.D., Fagoaga, A., Domínguez García, A.C., Alberdi, M.T., Bonini, R., Cerdeño, E., Denys, C., Domingo, L., Domingo, S., Gutiérrez, M.A., López-Cantalapiedra, J., Pesquero, M.D., Prado, J.L., Sevilla, P., Stöetzel, E., Tomassini, R.L., Fernández, F.J., 2021. New palaeoecological approaches to interpret climatic fluctuations in Holocene sites of the Pampean Region of Argentina. *Quat. Sci. Rev.* 255, 106816. <https://doi.org/10.1016/j.quascirev.2021.106816>.
- Garreaud, R.D., Vuille, M., Compagnucci, R., Marengo, J., 2009. Present-day south American climate. *Palaeogeogr. Palaeoclimatol. Palaeoecol.* 281, 180–195. <https://doi.org/10.1016/j.palaeo.2007.10.032>.
- Gasparini, G.M., Rabassa, J., Deschamps, C., Tonni, E.P. (Eds.), 2016. *Marine Isotope Stage 3 in Southern South America, 60 KA B.P.–30 KA B.P.* Springer Earth System Sciences. Springer International Publishing, Cham. <https://doi.org/10.1007/978-3-319-40000-6>.
- Gili, S., Gaiero, D.M., Goldstein, S.L., Chemale, F., Jweda, J., Kaplan, M.R., Becchio, R.A., Koester, E., 2017. Glacial/interglacial changes of Southern Hemisphere wind circulation from the geochemistry of South American dust. *Earth Planet. Sci. Lett.* 469, 98–109. <https://doi.org/10.1016/j.epsl.2017.04.007>.
- Glasser, N.F., Harrison, S., Winchester, V., Aniya, M., 2004. Late Pleistocene and holocene palaeoclimate and glacier fluctuations in Patagonia. *Global Planet. Change* 43, 79–101. <https://doi.org/10.1016/j.gloplacha.2004.03.002>.
- Gowan, E.J., Rovere, A., Ryan, D.D., Richiano, S., Montes, A., Pappalardo, M., Aguirre, M.L., 2021. Last interglacial (MIS 5e) sea-level proxies in southeastern South America. *Earth Syst. Sci. Data* 13, 171–197. <https://doi.org/10.5194/essd-13-171-2021>.
- Harrison, S.P., Prentice, I.C., 2003. Climate and CO₂ controls on global vegetation distribution at the last glacial maximum: analysis based on palaeovegetation data, biome modelling and palaeoclimate simulations. *Global Change Biol.* 9, 983–1004. <https://doi.org/10.1046/j.1365-2486.2003.00640.x>.
- Hayes, J.M., 2001. Fractionation of the isotopes of carbon and hydrogen in biosynthetic processes. In: Walley, John W.C., David, R. (Eds.), *Stable Isotope Geochemistry, Reviews in Mineralogy & Geochemistry*, pp. 225–277.
- Hernández Fernández, M., 2006. Rodent paleofaunas as indicators of climatic change in Europe during the last 125,000 years. *Quat. Res.* 65, 308–323. <https://doi.org/10.1016/j.yqres.2005.08.022>.
- Higgins, P., MacFadden, B.J., 2004. Amount Effect" recorded in oxygen isotopes of Late Glacial horse (*Equus*) and bison (*Bison*) teeth from the Sonoran and Chihuahuan deserts, southwestern United States. *Palaeogeogr. Palaeoclimatol.*

- Palaeoecol. 206, 337–353. <https://doi.org/10.1016/j.palaeo.2004.01.011>.
- Hoefs, J., 1997. *Stable Isotope Geochemistry*. Springer, Berlin.
- Huang, Y., Street-Perrott, F.A., Metcalfe, S.E., Brenner, M., Moreland, M., Freeman, K.H., 2001. Climate change as the dominant control on glacial-interglacial variations in C3 and C4 plant abundance. *Science* 293, 1647–1651. <https://doi.org/10.1126/science.1060143>.
- Huertas, A.D., Iacumin, P., Stenni, B., Chillón, B.S., Longinelli, A., 1995. Oxygen isotope variations of phosphate in mammalian bone and tooth enamel. *Geochim. Cosmochim. Acta* 59 (20), 4299–4305. [https://doi.org/10.1016/0016-7037\(95\)00286-9](https://doi.org/10.1016/0016-7037(95)00286-9).
- Hulton, N.R.J., Purves, R.S., McCulloch, R.D., Sugden, D.E., Bentley, M.J., 2002. The last glacial maximum and deglaciation in southern South America. *Quat. Sci. Rev.* 21, 233–241. [https://doi.org/10.1016/S0277-3791\(01\)00103-2](https://doi.org/10.1016/S0277-3791(01)00103-2).
- Hynek, S.A., Passey, B.H., Prado, J.L., Brown, F.H., Cerling, T.E., Quade, J., 2012. Small mammal carbon isotope ecology across the Miocene–Pliocene boundary, northwestern Argentina. *Earth Planet. Sci. Lett.* 321–322, 177–188. <https://doi.org/10.1016/j.epsl.2011.12.038>.
- Iriondo, M.H., García, N.O., 1993. Climatic variations in the Argentine plains during the last 18,000 years. *Palaeogeogr. Palaeoclimatol. Palaeoecol.* 101, 209–220. [https://doi.org/10.1016/0031-0182\(93\)90013-9](https://doi.org/10.1016/0031-0182(93)90013-9).
- Jackson, A.L., Inger, R., Parnell, A.C., Bearhop, S., 2011. Comparing isotopic niche widths among and within communities: SIBER – stable Isotope Bayesian Ellipses in R: Bayesian isotopic niche metrics. *J. Anim. Ecol.* 80, 595–602. <https://doi.org/10.1111/j.1365-2656.2011.01806.x>.
- Kershaw, A.P., Whitlock, C., 2000. Palaeoecological records of the last glacial-interglacial cycle: patterns and causes of change. *Palaeogeogr. Palaeoclimatol. Palaeoecol.* 155, 1–5. [https://doi.org/10.1016/S0031-0182\(99\)00091-7](https://doi.org/10.1016/S0031-0182(99)00091-7).
- Koch, P., Diffenbaugh, N.P., Hoppe, K.A., 2004. The effects of late Quaternary climate and pCO₂ change on C₄ plant abundance in the south-central United States. *Palaeogeogr. Palaeoclimatol. Palaeoecol.* 207, 331–357. <https://doi.org/10.1016/j.palaeo.2003.09.034>.
- Koch, P.L., 2007. Isotopic study of the biology of modern and fossil vertebrates. In: Michener, R., Lajtha, K. (Eds.), *Stable Isotopes in Ecology and Environmental Science*. Blackwell Publishing Ltd, Oxford, UK, pp. 99–154. <https://doi.org/10.1002/9780470691854.ch5>.
- Koch, P.L., 1998. Isotopic reconstruction of past continental environments. *Annu. Rev. Earth Planet. Sci.* 26, 573–613. <https://doi.org/10.1146/annurev.earth.26.1.573>.
- Kohfeld, K.E., Ridgwell, A., 2009. Glacial-interglacial variability in atmospheric CO₂. In: Le Quéré, C., Saltzman, E.S. (Eds.), *Geophysical Monograph Series*. American Geophysical Union, Washington, D. C., pp. 251–286. <https://doi.org/10.1029/2008GM000845>.
- Kohn, M.J., 2010. Carbon isotope compositions of terrestrial C₃ plants as indicators of (paleo)ecology and (paleo)climate. *Proc. Natl. Acad. Sci. Unit. States Am.* 107, 19691–19695. <https://doi.org/10.1073/pnas.1004933107>.
- Lopes, R.P., Ribeiro, A.M., Dillenburg, S.R., Schultz, C.L., 2013. Late middle to late Pleistocene paleoecology and paleoenvironments in the coastal plain of Rio Grande do Sul State, Southern Brazil, from stable isotopes in fossils of *Toxodon* and *Stegomastodon*. *Palaeogeogr. Palaeoclimatol. Palaeoecol.* 369, 385e394. <https://doi.org/10.1016/j.palaeo.2012.10.042>.
- Loponte, D., Corriale, M.J., 2020. Patterns of resource use and isotopic niche overlap among guanaco (*Lama guanicoe*), pampas deer (*Ozotoceros bezoarticus*) and marsh deer (*Blastoceros dichotomus*) in the pampas. *Ecological, paleoenvironmental and archaeological implications*. *Environ. Archaeol.* 25, 411–444. <https://doi.org/10.1080/14614103.2019.1585646>.
- Lüthi, D., Le Floch, M., Bereiter, B., Blunier, T., Barnola, J.-M., Siegenthaler, U., Raynaud, D., Jouzel, J., Fischer, H., Kawamura, K., Stocker, T.F., 2008. High-resolution carbon dioxide concentration record 650,000–800,000 years before present. *Nature* 453, 379–382. <https://doi.org/10.1038/nature06949>.
- Luz, B., Cormie, A.B., Schwarcz, H.P., 1990. Oxygen isotope variations in phosphate of deer bones. *Geochim. Cosmochim. Acta* 54, 1723–1728. [https://doi.org/10.1016/0016-7037\(90\)90403-8](https://doi.org/10.1016/0016-7037(90)90403-8).
- MacFadden, B.J., 2005. Diet and habitat of toxodont megaherbivores (mammalia, notoungulata) from the late quaternary of South and Central America. *Quat. Res.* 64, 113–124. <https://doi.org/10.1016/j.yqres.2005.05.003>.
- MacFadden, B.J., Shockey, B.J., 1997. Ancient feeding ecology and niche differentiation of Pleistocene mammalian herbivores from tarja, Bolivia: morphological and isotopic evidence. *Paleobiology* 23, 77–100.
- Marengo, J.A., Liebmann, B., Grimm, A.M., Misra, V., Silva Dias, P.L., Cavalcanti, I.F.A., Carvalho, L.M.V., Berbery, E.H., Ambrizzi, T., Vera, C.S., Saulo, A.C., Noguez-Paegle, J., Zipser, E., Seth, A., Alves, L.M., 2012. Recent developments on the South American monsoon system: recent developments on the south american monsoon system. *Int. J. Climatol.* 32, 1–21. <https://doi.org/10.1002/joc.2254>.
- Mayle, F.E., Beerling, D.J., Gosling, W.D., Bush, M.B., 2004. Responses of Amazonian ecosystems to climatic and atmospheric carbon dioxide changes since the last glacial maximum. *Philos. Trans. R. Soc. Lond. B Biol. Sci.* 359, 499–514. <https://doi.org/10.1098/rstb.2003.1434>.
- McGee, D., 2020. Glacial–interglacial precipitation changes. *Ann. Rev. Mar. Sci.* 12, 525–557. <https://doi.org/10.1146/annurev-marine-010419-010859>.
- Montalvo, C.I., Zárate, M.A., Bargo, M.S., Mehl, A., 2013. Registro Faunístico y Paleoambientes del Cuaternario Tardío, Provincia de la Pampa, Argentina. *Ameghiniana* 50, 554–570. <https://doi.org/10.5710/AMGH.21.09.2013.703>.
- Novello, V.F., Cruz, F.W., McGlue, M.M., Wong, C.I., Ward, B.M., Vuille, M., Santos, R.A., Jaquetto, P., Pessenda, L.C.R., Atorre, T., Ribeiro, L.M.A.L., Karmann, I., Barreto, E.S., Cheng, H., Edwards, R.L., Paula, M.S., Scholz, D., 2019. Vegetation and environmental changes in tropical South America from the last glacial to the Holocene documented by multiple cave sediment proxies. *Earth Planet. Sci. Lett.* 524, 115717. <https://doi.org/10.1016/j.epsl.2019.115717>.
- Ortiz-Jaureguizar, E., Cladera, G.A., 2006. Paleoenvironmental evolution of southern South America during the cenozoic. *J. Arid Environ.* 66, 498–532. <https://doi.org/10.1016/j.jaridenv.2006.01.007>.
- Otto-Bliessen, B.L., Rosenbloom, N., Stone, E.J., McKay, N.P., Lunt, D.J., Brady, E.C., Overpeck, J.T., 2013. How warm was the last interglacial? New model–data comparisons. *Philos. Trans. R. Soc. Math. Phys. Eng. Sci.* 371, 20130097. <https://doi.org/10.1098/rsta.2013.0097>.
- Pansani, T.R., Muniz, F.P., Cherkinsky, A., Pacheco, M.L.A.F., Dantas, M.A.T., 2019. Isotopic paleoecology (δ¹³C, δ¹⁸O) of late quaternary megafauna from mato grosso do Sul and Bahia States, Brazil. *Quat. Sci. Rev.* 221, 105864. <https://doi.org/10.1016/j.quascirev.2019.105864>.
- Passey, B.H., Robinson, T.F., Ayliffe, L.K., Cerling, T.E., Sponheimer, M., Dearing, M.D., Roeder, B.L., Ehleringer, J.R., 2005. Carbon isotope fractionation between diet, breath CO₂, and bioapatite in different mammals. *J. Archaeol. Sci.* 32, 1459–1470. <https://doi.org/10.1016/j.jas.2005.03.015>.
- Ponce, J.F., Rabassa, J., Coronato, A., Borromei, A.M., 2011. Paleogeographical evolution of the Atlantic coast of Pampa and Patagonia from the last glacial maximum to the Middle Holocene: paleogeography of patagonia since LGM. *Biol. J. Linn. Soc.* 103, 363–379. <https://doi.org/10.1111/j.1095-8312.2011.01653.x>.
- Prado, J.L., Martínez-Maza, C., Alberdi, M.T., 2015. Megafauna extinction in South America: a new chronology for the Argentine Pampas. *Palaeogeogr. Palaeoclimatol. Palaeoecol.* 425, 41–49. <https://doi.org/10.1016/j.palaeo.2015.02.026>.
- Prieto, A.R., 1996. Late quaternary vegetational and climatic changes in the Pampa grassland of Argentina. *Quat. Res.* 45, 73–88. <https://doi.org/10.1006/qres.1996.0007>.
- Quattrocchio, M.E., Borromei, A.M., Deschamps, C.M., Grill, S.C., Zavala, C.A., 2008. Landscape evolution and climate changes in the Late Pleistocene–Holocene, southern Pampa (Argentina): evidence from palynology, mammals and sedimentology. *Quat. Int.* 181, 123–138. <https://doi.org/10.1016/j.quaint.2007.02.018>.
- Rabassa, J., Coronato, A.M., Salemme, M., 2005. Chronology of the Late Cenozoic Patagonian glaciations and their correlation with biostratigraphic units of the Pampean region (Argentina). *J. South Am. Earth Sci.* 20, 81–103. <https://doi.org/10.1016/j.jsames.2005.07.004>.
- Rasmussen, S.O., Andersen, K.K., Svensson, A.M., Steffensen, J.P., Vinther, B.M., Clausen, H.B., Siggaard-Andersen, M.-L., Johnsen, S.J., Larsen, L.B., Dahl-Jensen, D., Bigler, M., Röthlisberger, R., Fischer, H., Goto-Azuma, K., Hansson, M.E., Ruth, U., 2006. A new Greenland ice core chronology for the last glacial termination. *J. Geophys. Res.* 111, D06102. <https://doi.org/10.1029/2005JD006079>.
- Ravibhanu, A., Katupotha, J., Aouitien, M., 2020. Comparative systematic analysis of Milankovitch cycles to identify variations of glaciers and interglacial periods of late Pleistocene in south asia. *TRIVALENT* *Archaeol. Tour. Anthropol.* 1, 1. <https://doi.org/10.4038/tjata.v1i1.24>.
- Richmond, G., Fullerton, D.S., 1986. Summation of quaternary glaciations in the United States of America. *Quat. Sci. Rev.* 5, 183–196. [https://doi.org/10.1016/S0277-3791\(86\)80018-X](https://doi.org/10.1016/S0277-3791(86)80018-X).
- Romero, M., Torre, G., Gaiero, D.M., 2021. Paleoenvironmental changes in southern South American dust sources during the last glacial/interglacial transition: evidence from clay mineral assemblages of the pampean loess. *Quat. Int.* 580, 11–21. <https://doi.org/10.1016/j.quaint.2020.12.044>.
- Rotti, A., Mothé, D., dos Santos Avilla, L., Semperebon, G.M., 2018. Diet reconstruction for an extinct deer (cervidae: cetartiodactyla) from the quaternary of South America. *Palaeogeogr. Palaeoclimatol. Palaeoecol.* 497, 244–252. <https://doi.org/10.1016/j.palaeo.2018.02.026>.
- Royer, T.C., Finney, B., 2020. An oceanographic perspective on early human migrations to the Americas. *Oceanography* 33 (1), 32–41.
- Sage, R.F., Wedin, D.A., Li, M., 1999. The biogeography of C₄ photosynthesis: patterns and controlling factors. *C4 plant biology* 10, 313–376.
- Sánchez, B., Prado, J.L., Alberdi, M.T., 2004. Feeding ecology, dispersal, and extinction of South American Pleistocene gomphotheres (gomphotheriidae, proboscidea). *Paleobiology* 30, 146–161.
- Siegenthaler, U., 2005. Stable carbon cycle-climate relationship during the late Pleistocene. *Science* 310, 1313–1317. <https://doi.org/10.1126/science.1120130>.
- Sigman, D.M., Boyle, E.A., 2000. Glacial/interglacial variations in atmospheric carbon dioxide. *Nature* 407, 859–869. <https://doi.org/10.1038/35038000>.
- Stirling, C.H., Esat, T.M., Lambeck, K., McCulloch, M.T., 1998. Timing and duration of the Last Interglacial: evidence for a restricted interval of widespread coral reef growth. *Earth Planet. Sci. Lett.* 160, 18. [https://doi.org/10.1016/S0012-821X\(98\)00125-3](https://doi.org/10.1016/S0012-821X(98)00125-3).
- Strömberg, C.A.E., 2011. Evolution of grasses and grassland ecosystems. *Annu. Rev. Earth Planet. Sci.* 39, 517–544. <https://doi.org/10.1146/annurev-earth-040809-152402>.
- Tejada-Lara, J.V., MacFadden, B.J., Bermudez, L., Rojas, G., Salas-Gismondí, R., Flynn, J.J., 2018. Body mass predicts isotope enrichment in herbivorous mammals. *Proc. R. Soc. B Biol. Sci.* 285, 20181020. <https://doi.org/10.1098/rspb.2018.1020>.
- Tipple, B.J., Pagani, M., 2007. The early origins of terrestrial C₄ photosynthesis. *Annu. Rev. Earth Planet. Sci.* 35, 435–461. <https://doi.org/10.1146/annurev.earth.35.031306.140150>.
- Tomassini, R.L., Montalvo, C.I., Garrone, M.C., Domingo, L., Ferigolo, J., Cruz, L.E.,

- Sanz-Pérez, D., Fernández-Jalvo, Y., Cerda, I.A., 2020. Gregariousness in the giant sloth *Lestodon* (xenarthra): multi-proxy approach of a bonebed from the last maximum glacial of Argentine pampas. *Sci. Rep.* 10, 10955. <https://doi.org/10.1038/s41598-020-67863-0>.
- Tonello, M.S., Prieto, A.R., 2008. Modern vegetation–pollen–climate relationships for the Pampa grasslands of Argentina. *J. Biogeogr.* 35, 926–938. <https://doi.org/10.1111/j.1365-2699.2007.01854.x>.
- Tonello, M.S., Prieto, A.R., 2010. Tendencias climáticas para los pastizales pampeanos durante el Pleistoceno tardío-Holoceno: estimaciones cuantitativas basadas en secuencias polínicas fósiles. *Ameghiniana* 47. <https://doi.org/10.5710/AMGH.v47i4.7>, 501–478.
- Tonni, E.P., Cione, A.L., Figini, A.J., 1999. Predominance of arid climates indicated by mammals in the pampas of Argentina during the Late Pleistocene and Holocene. *Palaeogeogr. Palaeoclimatol. Palaeoecol.* 147, 257–281. [https://doi.org/10.1016/S0031-0182\(98\)00140-0](https://doi.org/10.1016/S0031-0182(98)00140-0).
- Ward, D.J., Cesta, J.M., Galewsky, J., Sagredo, E., 2015. Late Pleistocene glaciations of the arid subtropical Andes and new results from the Chajnantor Plateau, northern Chile. *Quat. Sci. Rev.* 128, 98–116. <https://doi.org/10.1016/j.quascirev.2015.09.022>.
- Weaver, A.J., Saenko, O.A., Clark, P.U., Mitrovica, J.X., 2003. Meltwater pulse 1A from Antarctica as a trigger of the Bølling–Allerød warm interval. *Science* 299 (5613), 1709–1713. <https://doi.org/10.1126/science.1081002>.
- Whittaker, R.H., 1962. Classification of natural communities. *Bot. Rev.* 28, 1–239. <https://doi.org/10.1007/BF02860872>.
- Willez, M.-N., Kageyama, M., Krinner, G., de Noblet-Ducoudré, N., Viovy, N., Mancip, M., 2011. Impact of CO₂ and climate on the Last Glacial Maximum vegetation: results from the ORCHIDEE/IPSL models. *Clim. Past* 7, 557–577. <https://doi.org/10.5194/cp-7-557-2011>.
- Yehudai, M., Kim, J., Pena, L.D., Jaume-Seguí, M., Knudson, K.P., Bolge, L., Malinverno, A., Bickert, T., Goldstein, S.L., 2021. Evidence for a Northern Hemispheric trigger of the 100,000-y glacial cyclicity. *Proc. Natl. Acad. Sci. Unit. States Am.* 118. <https://doi.org/10.1073/pnas.2020260118>.
- Yu, J., Anderson, R.F., Rohling, E.J., 2014. Deep ocean carbonate chemistry and glacial-interglacial atmospheric CO₂ changes. *Oceanography* 27 (1), 16–25. <http://www.jstor.org/stable/24862115>.